

# Chromatin modification of Notch targets in olfactory receptor neuron diversification

Keita Endo<sup>1</sup>, M Rezaul Karim<sup>2,6</sup>, Hiroaki Taniguchi<sup>2,6</sup>, Alena Krejci<sup>3-5</sup>, Emi Kinameri<sup>2</sup>, Matthias Siebert<sup>2</sup>, Kei Ito<sup>1</sup>, Sarah J Bray<sup>3</sup> & Adrian W Moore<sup>2</sup>

Neuronal-class diversification is central during neurogenesis. This requirement is exemplified in the olfactory system, which utilizes a large array of olfactory receptor neuron (ORN) classes. We discovered an epigenetic mechanism in which neuron diversity is maximized via locus-specific chromatin modifications that generate context-dependent responses from a single, generally used intracellular signal. Each ORN in *Drosophila* acquires one of three basic identities defined by the compound outcome of three iterated Notch signaling events during neurogenesis. Hamlet, the *Drosophila* Evi1 and Prdm16 proto-oncogene homolog, modifies cellular responses to these iteratively used Notch signals in a context-dependent manner, and controls *odorant receptor* gene choice and ORN axon targeting specificity. In nascent ORNs, Hamlet erases the Notch state inherited from the parental cell, enabling a modified response in a subsequent round of Notch signaling. Hamlet directs locus-specific modifications of histone methylation and histone density and controls accessibility of the DNA-binding protein Suppressor of Hairless at the Notch target promoter.

Neuronal-class diversification mechanisms are fundamental to neurogenesis. For example, the mammalian retina utilizes around 60 neuron classes and our cortex utilizes over 1,000 (ref. 1). The olfactory system requires approximately 1,200 ORN classes in the mouse and 50 in *Drosophila*<sup>2-5</sup>. Each ORN class is tuned to particular odors via expression of specific odorant receptors, and sends axons that converge to a class-specific glomerulus in the primary olfactory center<sup>2-5</sup>.

*Drosophila* ORNs are housed in at least 21 different types of hair-shaped sensilla, each of which typically contains two or three ORNs in invariant class combinations<sup>2-4</sup>. An important mechanism for diversifying *Drosophila* ORNs is the canonical Notch pathway, a broadly used, evolutionarily conserved signaling system<sup>6,7</sup>. ORNs in a sensillum are a clonal set derived from a single sensory organ precursor (SOP) cell in a stereotypic lineage (Fig. 1a)<sup>8</sup>. An SOP divides asymmetrically, creating two intermediate precursor cells, pIIa and pIIb, which produce non-neural and neural components of the sensilla, respectively. The neural-intermediate precursor (pIIb) divides asymmetrically again to produce a second set of intermediate precursors, pNa and pNb.

During both asymmetric divisions, Numb protein and its adaptor protein Partner of Numb (Pon) are asymmetrically segregated to one of the two daughters. Notch signaling is repressed by Numb in one daughter, but is activated in the other. This binary difference in Notch activity produces two different cell fates. According to the traditional model, the sequence-specific DNA-binding protein Suppressor of Hairless (Su(H)) recruits a co-repressor complex to the promoters of Notch targets in cells in which Notch signaling is suppressed and maintains them in a silent state. In cells in which Notch signaling is activated, the Notch intracellular domain (NICD)

translocates to the nuclei, where it binds to Su(H), displaces co-repressors and recruits co-activators, and the resultant complex activates Notch target genes<sup>6,9</sup>.

The manner by which pNa and pNb intermediate precursors generate up to four different classes of ORNs remains unknown<sup>8</sup>. We found that pNa and pNb also divide asymmetrically, each generating two different cell fates. Thus, ORNs are diversified by the output of three iterative Notch-mediated binary cell fate decisions.

Given the simplicity of the Notch signal transduction response, these Notch signaling events must be modified in a context-dependent manner to generate multiple outcomes. Such modification typically occurs at the level of Notch target transcriptional control<sup>9</sup> via combinatorial integration of transcription factors with the NICD or Su(H) at Notch target enhancers. These factors act either as combinatorial co-activators or to relieve default repression by the Su(H) complex<sup>9-12</sup>. Here, however, we examined a previously unknown epigenetic mechanism that modifies Notch signaling.

We found that the *Hamlet* (*Ham*), the *Drosophila* homolog of mammalian Evi1 (Ecotropic viral integration 1, also known as Mecom) and *Prdm16* (PRDI-BF1 and RIZ homology domain containing 16) proto-oncogenes<sup>13-15</sup>, was expressed only in the pNa sublineage and specified pNa-derived ORN identities. By analyzing the interaction of Ham with *Enhancer of split* (*E(spl)*) loci, we found that Ham acts to direct chromatin-modification events at specific Notch targets, altering the accessibility for Su(H) binding at the enhancer. In nascent ORNs, Ham activity erased the Notch state that was inherited from the parental pNa intermediate precursor cell. This permitted a new and modified response of Notch targets in the subsequent

<sup>1</sup>Institute of Molecular and Cellular Biosciences, The University of Tokyo, Bunkyo-ku, Tokyo, Japan. <sup>2</sup>Disease Mechanism Research Core, RIKEN Brain Science Institute, Wako, Saitama, Japan. <sup>3</sup>Department of Physiology, Development, and Neuroscience, University of Cambridge, Cambridge, UK. <sup>4</sup>Faculty of Science, University of South Bohemia, Ceske Budejovice, Czech Republic. <sup>5</sup>Institute of Entomology, Biology Centre of the Academy of Sciences of the Czech Republic, Ceske Budejovice, Czech Republic. <sup>6</sup>These authors contributed equally to this work. Correspondence should be addressed to A.W.M. (adrianm@brain.riken.jp).

Received 4 September; accepted 31 October; published online 25 December 2011; doi:10.1038/nn.2998

round of Notch signaling. The outcome was the maximization of ORN class output from a single neurogenic lineage.

## RESULTS

### Iterated asymmetric cell divisions diversify ORN classes

The two progeny of the pIIb, pNa and pNb, divide to produce four cells. Among them, typically three (occasionally four) cells became neurons, which were stained with a pan-neuronal Elav (embryonic lethal abnormal vision) antibody (Fig. 1a,b). Asymmetric localization of a Pon-Numb complex drives a subsequent asymmetry in Notch signaling during the first two divisions of the ORN lineage<sup>8</sup>, and we

examined whether this also occurs during the pNa and pNb divisions by following the localization of Pon<sup>8,16</sup> in MARCM (mosaic analysis with a repressible cell marker) clones (Online Methods). As in the first and second cell divisions of the ORN lineage, we observed asymmetric segregation of Pon between the daughter cells of both pNa and pNb (Fig. 1a,b). Thus, the ORNs in a single sensillum are generated by three iterated rounds of Notch-mediated asymmetric divisions and can be individually discriminated via their lineage and inheritance of Pon.

We named each cell using nomenclature similar to *Drosophila* external sensory organ lineages, where 'a' is added to the name of a

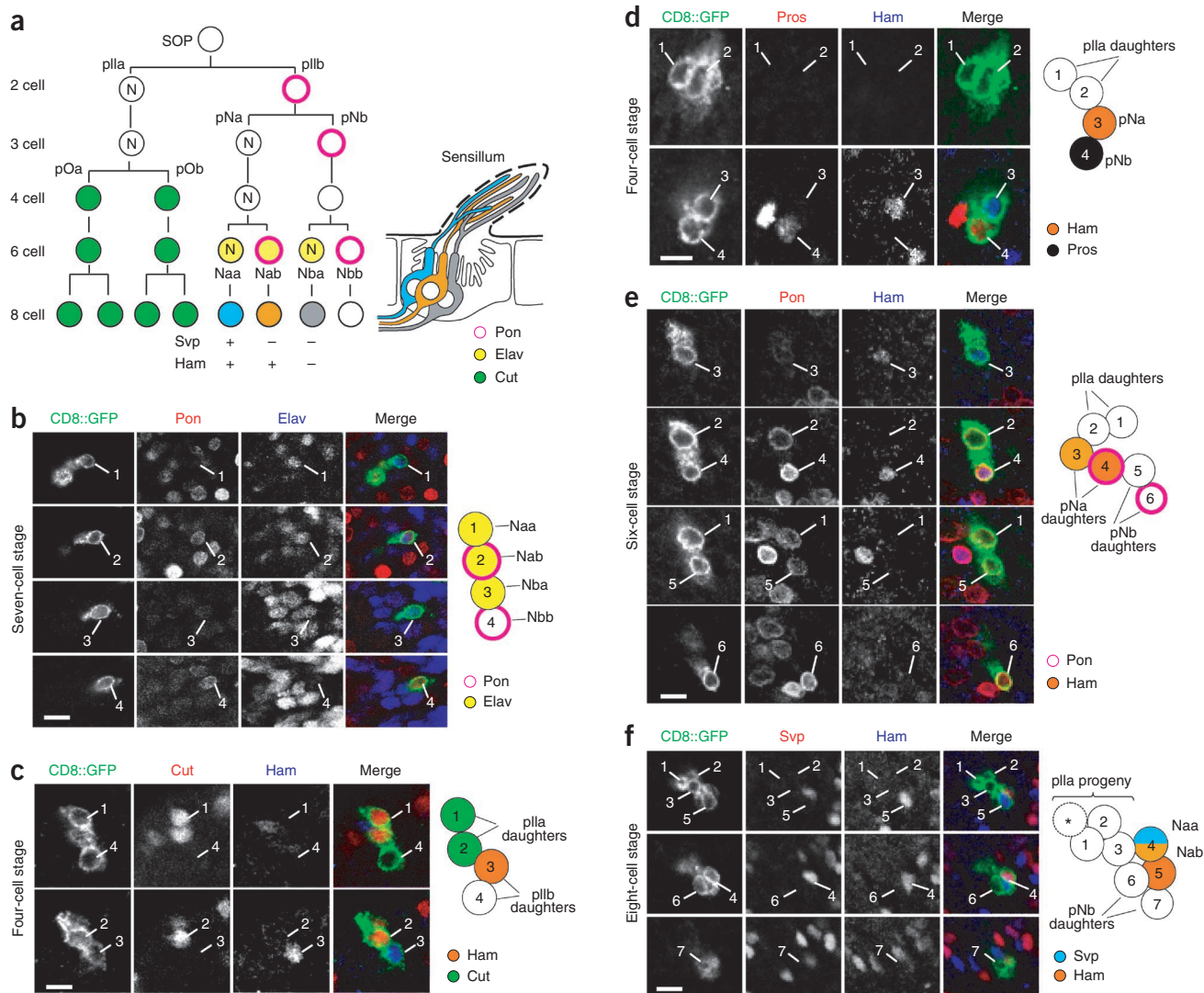


**Figure 1** Differential Notch signaling and Ham and Svp expression delineates ORN identity. **(a)** 3-ORN sensillum lineage. Cut marks non-neural pIIa progeny. In the neural lineage, Pon is asymmetric at each stage (N, high Notch activity). Pan-neuronal Elav marks three ORNs, each differentially expressing Ham, Svp and Pon. pNa divides before pNb, and pOa and pOb cells also divide asynchronously, producing transient five- and seven-cell stages (not shown). **(b–f)** Wild-type MARCM clones derived from a single SOP, immunostained for GFP (green) and other cell type-specific markers. Rows in each panel represent different apico-basal focal planes of the pupal antenna. Each individual cell in the immunostained MARCM clone is indicated with a number and is represented by the same number in the accompanying summary diagram. Scale bars represent 5  $\mu$ m. **(b)** Seven-cell stage clone. Pon is shown in red and Elav in blue. Pon was expressed on one Elav-positive and one Elav-negative cells. pIIa progeny do not form neurons and are not shown. Cell identity was assigned by stereotypic position along the apico-basal axis and by integrating information from **c–f** and **Supplementary Figure 1**. **(c)** Four-cell stage clone. Cut is shown in red and Ham in blue. Cut marks the outer cells derived from pIIa. Ham was expressed in one of the Cut-negative pIIb daughters. **(d)** Four-cell stage clone. Pros is shown in red and Ham in blue. Ham was expressed in the Pros-negative pNa cell. **(e)** Six-cell stage clone. Pon is shown in red and Ham in blue. Ham was expressed in one Pon-positive and one Pon-negative cell. **(f)** Eight-cell stage clone. Svp is shown in red and Ham in blue. Svp was expressed in the cell that showed weaker Ham staining than its sibling. \*One pIIa progeny is out of the focal plane.

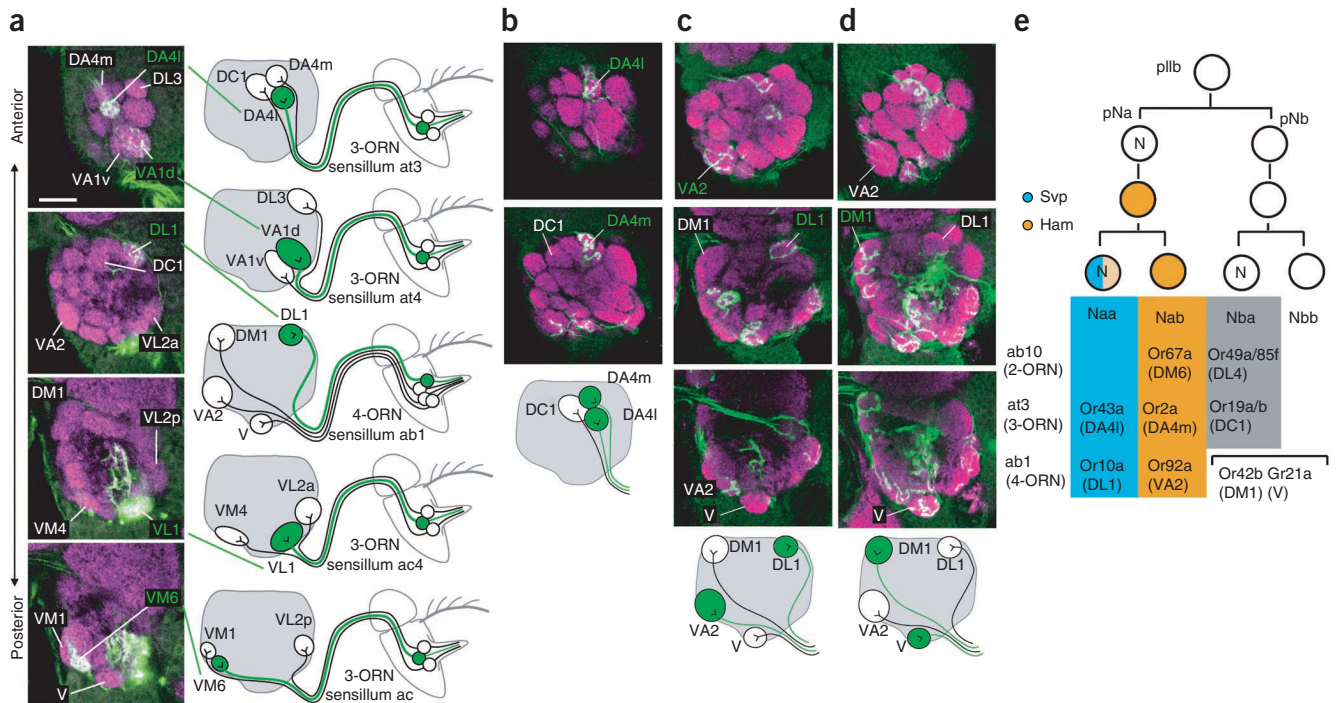


**Figure 2** Naa, Nab and Nba identities in the ORN lineage. **(a)** Axonal projections of the wild-type ORN clones labeled by *GAL4-NP0724*. Left, different focal planes of an antennal lobe along the antero-posterior axis. Only five glomeruli DA4I, VA1d, DL1, VL1 and VM6 were innervated by the clone. Each of these glomeruli was the projection target of one of the ORNs in the 3-ORN and 4-ORN sensilla, as shown in the schematics on the right. Scale bar represents 20  $\mu$ m. **(b–d)** Axonal projection of wild-type clones that were labeled by pan-neuronal *Gal4-C155* and induced at a late stage of the ORN lineage. Panels in each column represent different focal planes of an antennal lobe. Only two of the three target glomeruli of ORNs in the at3 sensillum (DA4m and DA4I) and two of the four target glomeruli of ORNs in the ab1 sensillum (VA2 and DL1 or DM1 and V) were co-innervated by the labeled clone, as shown in the schematics at the bottom. **(e)** Representation of the ORN lineage for ab10, at3 and ab1 sensilla. The odorant receptors expressed and glomerulus innervated by each ORN in the sensilla are indicated.

cell with high Notch activity and 'b' to one with low Notch activity: Naa (pNa derived, Pon<sup>-</sup>, Notch<sup>+</sup> and Elav<sup>+</sup>), Nab (pNa derived, Pon<sup>+</sup>, Notch<sup>-</sup> and Elav<sup>+</sup>), Nba (pNb derived, Pon<sup>-</sup>, Notch<sup>+</sup> and Elav<sup>+</sup>) and Nbb (pNb derived, Pon<sup>+</sup>, Notch<sup>-</sup> and Elav<sup>-</sup>) (**Fig. 1a**).

### A subset of terminal ORN lineage divisions expresses Ham

How can repeated use of the same Notch-mediated asymmetric division machinery generate multiple ORN classes? This may occur via context-dependent transcriptional control. We surveyed transcriptional regulators that are active in embryonic neurogenesis for expression in the antenna during olfactory neurogenesis. From this, we found that the Prdm factor Ham<sup>14</sup> was expressed in the ORN lineage.

We examined Ham expression via antibody staining in MARCM clones at sequential stages during lineage elaboration (Online Methods). Ham was not expressed in the SOP and at the two- or three-cell stages of the ORN lineage. At the four-cell stage, Ham expression was initiated in one Cut-negative, Prospero (Pros)-negative cell (**Fig. 1c,d**). Because Cut marked cells derived from pIIa, and Pros marked the pIIb-derived pNb (**Supplementary Fig. 1a,b**)<sup>8</sup>, the Ham-positive cell is pNa. Ham was expressed in both pNa daughters (Naa and Nab; **Fig. 1e**), along with the pan-neuronal marker Elav (**Supplementary Fig. 1b,c**). Ham expression was then lost before terminal differentiation (**Supplementary Fig. 2**). Given that Ham is expressed specifically in pNa and its daughters Naa and Nab, Ham fits the expression criteria for a sublineage-specific modifier of Notch signaling.

In addition to Ham, Seven-up (Svp) is expressed in one terminal cell in the ORN lineage<sup>8</sup>. We used Ham and Svp in combination to dissect Naa, Nab and Nba identities. Immediately following

division of pNa (the six-cell stage), there was a consistent small ( $16 \pm 3\%$ , mean  $\pm$  s.e.m.,  $n = 6$ ) difference in Ham expression between Naa and Nab cells (**Supplementary Fig. 2**). Ham expression subsequently declined at an equal rate in both cells. The difference in Ham expressed between Naa and Nab cells remained in 96% ( $n = 27$ ) of late-stage *numb* clones<sup>8</sup>, suggesting that it is generated independently of asymmetric Notch activation between Naa and Nab cells. At the eight-cell stage, Svp expression was always initiated in the ORN with the slightly weaker Ham labeling, which was Naa (**Fig. 1f**). Consequently, the three ORN identities derived from a single SOP (Naa, Nab and Nba) were characterized by different combinations of Ham and Svp (**Fig. 1a**).

### ORN classes formed by Naa, Nab and Nba

There are at least 21 different types of sensilla, each with a specific complement of ORN classes. We investigated the relationships between the stereotypic Naa, Nab and Nba ORN identities and the ORN classes that compose each type of sensillum. There are usually two (2-ORN) or three (3-ORN) ORNs in a sensillum. In addition, a few types of sensilla contain only a single ORN (1-ORN), and one sensillum contains four ORNs (4-ORN). MARCM clones at the eight-cell stage contained three Elav-positive cells, and never contained only one or two. This suggests that, in 1-ORN or 2-ORN sensilla, three Elav-positive cells initially form and then a subset dies or adopts a non-ORN fate. In rare cases, we detected four Elav-positive cells; these are likely to be clones in the 4-ORN sensillum ab1.

Svp was expressed in Naa (**Fig. 1a,f**). We therefore used *Gal4-NP0724*, an enhancer trap in the *svp* promoter<sup>17</sup> that accurately

**Table 1 Summary of Naa, Nab and Nba identities, and *ham* phenotypes on ORN axonal projections**

Sensilla type		Odorant receptor class	Innervating glomerulus	<i>NPO724 &gt; mCD8::GFP</i>	Clonal analysis*	Innervation in <i>ham</i> ***	Identity	
Antennal trichoid	at1	<i>Or67d</i>	DA1	–	N.D.	None	Nab?	
	at2	<i>Or83c</i>	DC3	–	N.D.	1/8	Nab	
		<i>Or23a</i>	DA3	–		8/8	Nba	
	at3	<i>Or43a</i>	DA4l	+	3/35	3/6	Naa	
		<i>Or2a</i>	DA4m	–		0/6	Nab	
	at4	<i>Or19a/b</i>	DC1	–	4/35	6/6	Nba	
		<i>Or88a</i>	VA1d	+	1/35	2/8	Naa	
		<i>Or47b</i>	VA1v	–		0/8	Nab	
	Antennal intermediate	ai1	<i>Or65a/b/c</i>	DL3	–	1/35	8/8	Nba
				VA7m	–	N.D.	0/5	Nab
Antennal basiconica	ab1	<i>Or13a</i>	DC2	–		5/5	Nba	
		<i>Or10a</i>	DL1	+	5/35	0/9	Naa	
Maxillary palp basiconica	pb1	<i>Or92a</i>	VA2	–		0/9	Nab	
		<i>Or42b</i>	DM1	–	5/35	9/9	Nba	
	ab2	<i>Gr21a</i>	V	–		9/9	Nbb	
		<i>Or85a</i>	DM5	–	N.D.	0/5	Nab	
	ab3	<i>Or59b</i>	DM4	–		5/5	Nba	
		<i>Or85b</i>	VM5d	–	N.D.	0/8	Nab	
	ab4	<i>Or22a/b</i>	DM2	–		8/8	Nba	
		<i>Or56a</i>	DA2	–	N.D.	0/7	Nab	
	ab5	<i>Or7a</i>	DL5	–		7/7	Nba	
		<i>Or82a</i>	VA6	–	N.D.	0/9	Nab	
ab6	<i>Or47a</i>	DM3	–		9/9	Nba		
	<i>Or49b</i>	VA5	–	N.D.	7/7	Nba?		
ab7	<i>Or98a</i>	VM5v	–	N.D.	1/7	Nab		
	<i>Or67c</i>	VC4	–		5/7	Nba		
ab8	<i>Or43b</i>	VM2	–	N.D.	1/9	Nab		
	<i>Or9a</i>	VM3	–		8/9	Nba		
ab9	<i>Or67b</i>	VA3	–	N.D.	6/9	Nab?		
	<i>Or69aA/aB</i>	D	–		8/9	Nba		
ab10	<i>Or67a</i>	DM6	–	N.D.	0/8	Nab		
	<i>Or49a/85f</i>	DL4	–		8/8	Nba		
Antennal coeloconica**	ac	<i>Or42a</i>	VM7d(VM7)	–	N.D.	1/6	Nab	
		<i>Or71a</i>	VC2	–		6/6	Nba	
	pb2	<i>Or46a</i>	VA7l	–	N.D.	0/7	Nab	
<i>Or33c/85e</i>		VC1	–		7/7	Nba		
ac3	<i>Or59c</i>	<i>Or59c</i>	VM7v(1)	–	N.D.	2/7	Nab	
		<i>Or85d</i>	VA4	–		7/7	Nba	
ac4	<i>Or35a</i>	VM6	+	7/35	3/5	Naa		
		VL2p	–		0/5	Nab		
ac4	<i>IR76a/b</i>	VM1	–	2/35	5/5	Nba		
		DL2	–	N.D.	4/6	Nab?		
ac4	<i>IR76a/b</i>	VC3	–		6/6	Nba		
		VL1	+	2/35	0/6	Naa		
ac4	<i>IR76a/b</i>	VL2a	–		0/6	Nab		
		VM4	–	4/35	6/6	Nba		

A table showing a cross-sensilla-type summary of ORN class labeled by *Gal4-NPO724* (Naa), sibling analysis (for a subset of sensilla) and axonal projection defects in *ham* mutants. On the basis of these results, the Naa, Nab and Nba identities of different ORN classes were determined. \*Colabeling was seen only for the two glomeruli indicated here for each sensilla, except for an undetermined sensillum that we refer to as ac. In this sensillum, we found two different sets of colabeled neurons; VL2p and VM1 were colabeled in 2 of 35 sensillum, and VM6 and VM1 were colabeled in 4 of 35 sensillum. \*\*Data for some neuron classes housed in the antennal coeloconica were not included. \*\*\*Frequencies of concurrent projections of *ham* clones to specific glomeruli are shown. The denominator represents the number of samples in which at least one of the target glomeruli of ORNs in a given sensillum was innervated. The numerator represents the number of samples in which the target glomerulus of a given ORN class was innervated. N.D., not done.

labels the Svp-positive neurons (Supplementary Fig. 3), to visualize the axonal projections of Naa in the antennal lobe. Svp-positive Naa ORNs innervated only a small subset of glomeruli: DA4l, VA1d, DL1, VL1 and VM6 (Fig. 2a). Each of these glomeruli are the projection targets of one ORN housed in 3-ORN or 4-ORN sensilla<sup>3,4,8</sup>. Thus, Naa became an ORN only in 3-ORN and 4-ORN sensilla (Table 1).

To investigate the ORN class identities of Nab, we analyzed which classes are immediate siblings of the Naa ORNs. We induced wild-type MARCM clones at a late stage of ORN lineage elaboration such that the labeled clones mostly consisted of pairs of ORNs that were daughters of

either pNa or pNb<sup>8</sup>. Analyzing the glomeruli pairs that received the axonal projection from such clones, we identified pairs of Naa and Nab ORNs only in 3-ORN and 4-ORN sensilla (Table 1). In the 3-ORN sensillum called at3, the ORNs innervating DA4l and DA4m were colabeled, whereas the ORN innervating DC1 was never colabeled with another neuron (Fig. 2b and Table 1). Because the ORN innervating DA4l was the Svp-positive Naa, the cell that innervated DA4m was its direct sibling Nab, and the remaining ORN innervating DC1 was Nba (Fig. 1a). In the 4-ORN sensillum ab1, ORNs innervating DL1 and VA2 were colabeled (Fig. 2c and Table 1). As the ORN innervating DL1 was Naa, then the ORN innervating VA2 was Nab (Fig. 1a). ORNs innervating DM1 and V were also colabeled (Fig. 2d and Table 1) and were the daughters of pNb (Fig. 2e). In the 2-ORN sensillum, where the Svp-positive cell does not form an ORN, the identities of the Nab and Nba cells were determined by the effects of *ham* loss of function.

For each type of sensillum, the members of each stereotypic ORN identity (that is, Naa, Nab and Nba) can be identified based on the neuronal projection pattern in the antennal lobe (Fig. 2e). Thus, analysis of projections can be used to distinguish perturbations in ORN fate specification.

### Ham controls axonal targeting

Is Ham required for the specification of ORN classes? We generated MARCM clones homozygous for *ham* and analyzed axonal projections of the mutant ORN in the antennal lobe. Ham was required for the axonal projection of Naa and Nab in 3-ORN and 4-ORN sensilla (Fig. 3a,b and Table 1). For example, in the 3-ORN at3, *ham*<sup>-/-</sup> clones failed to project to DA4l and DA4m, the targets of Naa and Nab, respectively. On the other hand, *ham*<sup>-/-</sup> clones projected normally to DC1, the target of Nba (Fig. 3a). In the 4-ORN ab1, *ham*<sup>-/-</sup> clones failed to project to DL1 and VA2, the targets of Naa and Nab. However, the other two ORNs projected normally to DM1 and V (Fig. 3b). In the 2-ORN sensilla, the axonal projection of one of the ORNs was disrupted in *ham*<sup>-/-</sup> clones

(Table 1). For example, in ab10, the projection to DM6 was disrupted, whereas that to DL4 was unaffected (Fig. 3c). As the Svp-positive Naa does not form an ORN in the 2-ORN sensilla, the two ORNs must be Nab (Ham positive) and Nba (Ham negative). Given that Ham function has been suggested to be cell autonomous<sup>14,15,18</sup>, the ORN affected by *ham* mutation in the 2-ORN sensillum should be Nab (Fig. 2e and Table 1).

To examine Ham activity at a single-sensillum level, we used *Gal4-AM29*, which specifically labels only the two ORNs of ab10 (Fig. 3d)<sup>8</sup>. *Gal4-AM29*-labeled ORNs in *ham*<sup>1/Df(2L)ED1195</sup> flies showed loss

**Figure 3** *ham* mutant ORNs switch axonal projection identities. (a,b) Axonal projection of the *ham* clones labeled by pan-neuronal *Gal4-C155*. The panels in each row represent different focal planes of an antennal lobe. The mutant clones failed to project to DA4I and DA4m (a) and to DL1 and VA2 (b), the target glomeruli of Naa and Nab ORNs, of the at3 sensillum and of the ab1 sensillum, respectively. (c) *ham* mutant clones failed to project DM6, the target glomerulus of Nab ORN in the ab10 sensillum. (d) Axonal projection of the wild-type clones of the *Gal4-AM29*-labeled ORNs in ab10 sensillum to DM6 and DL4. (e) *ham* clones failed to arborize at the DM6 glomerulus and projected further toward DL4. Scale bar represents 20  $\mu$ m.

of targeting to DM6, but not to DL4 (Supplementary Fig. 4a,b). Similarly, in *ham*<sup>-/-</sup> clones, axonal projections to DL4 were always present ( $n = 19$ ), whereas those to DM6 were altered in 74% of the clones. Of this 74%, projections to DM6 were completely lost in 21% of clones, two axons from the sensillum projected to DL4 in 16% of the clones, but none projected to DM6, and in 37% of the clones, axons initially projected toward DM6, but then branched to ectopic locations including DL4 (Fig. 3e). Thus, in *ham* mutants, ORN axonal-targeting identity is fully or partially converted from Nab to Nba.

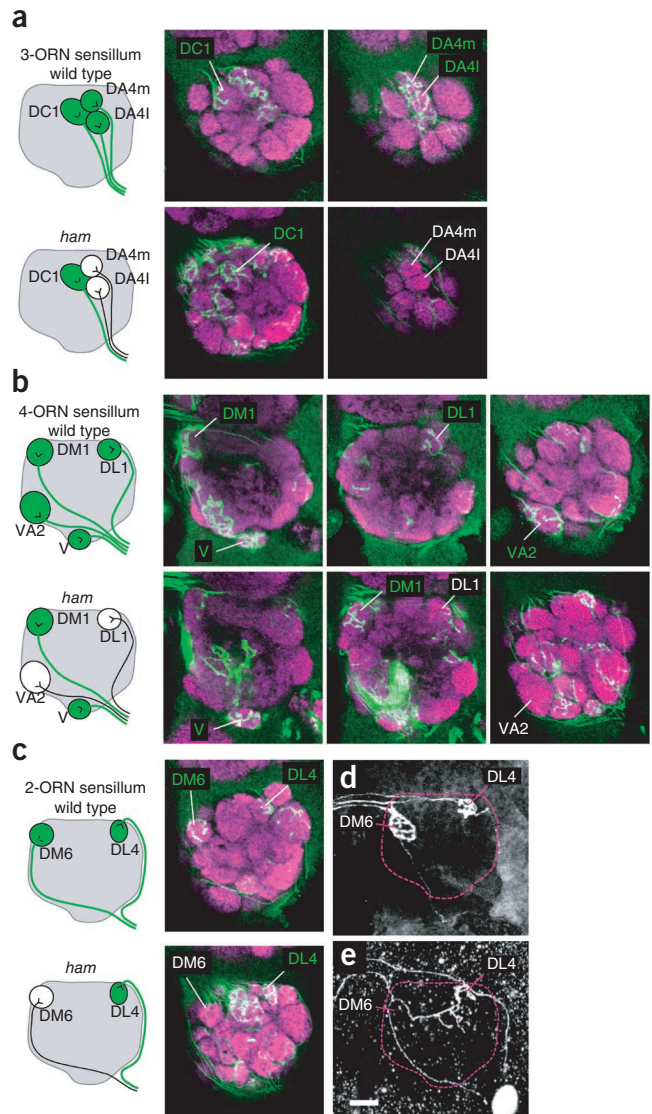
### Ham directs odorant receptor expression

Given that ORN class specification involves not only axonal projection targeting, but also odorant receptor selection, we next analyzed odorant receptor expression in *ham*<sup>-/-</sup> antenna. In the at3 3-ORN sensillum, Naa, Nab and Nba ORNs expressed the odorant receptors *Or43a*, *Or2a*, and *Or19a* and *Or19b*, respectively (Fig. 2e). We labeled these ORNs using *Or43a-mCD8::GFP*, *Or2a-mCD8::GFP* and *Or19a-mCD8::GFP* transgenes<sup>3</sup> and counted the number of each ORN class in wild-type and *ham*<sup>-/-</sup> antenna. In *ham*<sup>-/-</sup> antenna, the number of *Or43a*-expressing neurons was the same as wild type (Fig. 4a). However, the numbers of *Or2a*-expressing neurons were greatly reduced by 99.7% (Fig. 4a,b) and those expressing *Or19a* increased by 121% (Fig. 4a,c). In addition, in *ham*<sup>-/-</sup> antenna, we frequently observed duplicated *Or19a*-expressing neurons in a single sensillum (Fig. 4d). Similarly, in the 2-ORN sensillum ab10, in which Nab and Nba ORNs express *Or67a* and *Or49a*, respectively (Fig. 2e), *ham* mutation resulted in a 70% reduction in the number of *Or67a*-expressing neurons and a 58% increase in the number of neurons expressing *Or49a* (Fig. 4a). These data suggest that *ham* mutation switches odorant receptor expression from Nab to Nba identity.

To test whether Ham is instructive for odorant receptor selection, we overexpressed Ham in the ORN lineage (*neur>ham*, *tub-Gal80<sup>ts</sup>*, see Online Methods). The effect of ectopic Ham expression on odorant receptor selection was the opposite of that of the loss-of-function phenotype, a 38% increase and 27% decrease in *Or67a*- and *Or49a*-expressing neurons, respectively (Fig. 4a). This suggests that Ham instructs the odorant receptor selection from Nba to Nab identity and manages both axon target selection and odorant receptor gene choice.

### Ham modifies Notch activity

What relationship exists between Ham activity and Notch signaling? In *Drosophila* microchaete sensory organs, a Notch-mediated binary cell-fate choice between the hair (with low Notch signal) and the socket cell (with high Notch signal) is a well-characterized system for investigating the regulation of Notch activity<sup>19,20</sup> (Fig. 5a). To assay interactions of Ham and Notch, we ectopically expressed Ham in microchaete organs using the weak *Gal4-109-68* driver<sup>20</sup>. This resulted in sense organs containing either socket cells with ectopic hair



shaft-like structures, or two complete hairs and no socket (Fig. 5a). These phenotypes are consistent with ectopic Ham disrupting Notch and *Su(H)* activity in the socket cell<sup>19</sup>.

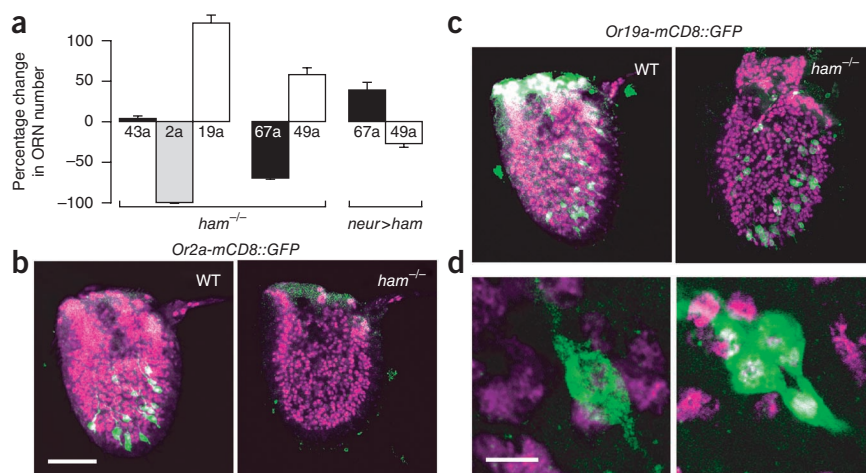
To verify the involvement of Notch in this phenotype, we assessed whether reducing Notch activity by removing one copy of the *Notch* gene enhances the phenotypes caused by ectopic *ham* (*N<sup>+/-</sup>; Gal4-109-68>ham*). This resulted in an increase in the proportion of socket cells that were partially transformed to hair fate and, in particular, of those that contained two hairs and no socket (Fig. 5b and Supplementary Fig. 5a). A similar interaction was also seen when removing one copy of *Su(H)* (Supplementary Fig. 5a). These data suggest that Ham suppresses Notch and *Su(H)* activity.

### Ham recruits CtBP

To examine the molecular mechanism of Ham action, we screened for proteins that interact with Ham in a native complex. We carried out immunoprecipitation of V5-tagged Ham protein expressed in *Drosophila* S2 cells and analyzed the precipitated complex by liquid chromatography-mass spectrometry followed by a Mascot search (Online Methods). Using a  $P < 0.05$  cut-off, we found that the transcriptional co-repressor C-terminal binding protein (CtBP) was present in a complex with Ham. To confirm this interaction, we found

**Figure 4** Ham acts as a switch between Nab and Nba odorant receptor expression identity.

(a) A bar chart showing the percentage change in a given ORN class in *ham* mutants or in flies with ectopic *ham* expression (*neur>ham*). Data is shown as mean  $\pm$  s.e.m. For each experiment, a probability was determined by unpaired, two-tailed Student's *t* tests. For *ham* loss-of-function, we examined *Or43a* (wild type (WT),  $n = 11$ ; *ham*,  $n = 8$ ;  $P = 0.14$ ), *Or2a* (wild type,  $n = 5$ ; *ham*,  $n = 15$ ;  $P = 2.1 \times 10^{-24}$ ), *Or19a* (wild type,  $n = 6$ ; *ham*,  $n = 6$ ;  $P = 5.8 \times 10^{-7}$ ), *Or67a* (wild type,  $n = 6$ ; *ham*,  $n = 3$ ;  $P = 4.2 \times 10^{-8}$ ) and *Or49a* (wild type,  $n = 6$ ; *ham*,  $n = 5$ ;  $P = 0.00033$ ) expression. For *ham* ectopic expression, we examined *Or67a* (wild type + heat shock,  $n = 4$ ; *neur>ham* + heat shock,  $n = 16$ ;  $P = 0.00043$ ) and *Or49a* (wild type + heat shock,  $n = 11$ ; *neur>ham* + heat shock,  $n = 16$ ;  $P = 0.00023$ ). (b,c) Whole-mount antennae of wild-type and *ham<sup>-/-</sup>Df(2L)ED1195* flies immunostained for the neuronal marker Elav (magenta) and GFP (green) to show the expression of a given *Or-mCD8::GFP* reporter. Scale bar represents 50  $\mu$ m and applies to both b and c. *Or2a-mCD8::GFP*-expressing neurons were lost (b) and *Or19a-mCD8::GFP*-expressing neurons were gained in the b *ham<sup>-/-</sup>* antenna (c). (d) *Or19a-mCD8::GFP* expression in a single sensillum, showing duplication of *Or19a*-expressing neurons in the *ham<sup>-/-</sup>* antenna. Scale bar represents 5  $\mu$ m.



that *Drosophila* CtBP and Ham were co-immunoprecipitated when coexpressed in S2 cells (Supplementary Fig. 5c).

Comparison of the protein domain structure of Ham and its homologs Evi1, Prdm16 and Egl43 identified a conserved canonical binding site for CtBP (PLDLS at amino acids 747–751; Fig. 5c,d). Both Evi1 and Prdm16 bind CtBP through this sequence to repress gene transcription<sup>21–23</sup>. GST-pulldown experiments revealed strong CtBP–Ham binding (Fig. 5e and Supplementary Fig. 6), which was lost when the PLDLS sequence was mutated to a nonfunctional PLASS sequence (Ham $\Delta$ CtBP; Fig. 5f and Supplementary Figs. 5d and 6)<sup>22,23</sup>.

We assayed whether Notch signaling suppression by Ham in microchaete organs can be altered by disrupting the Ham–CtBP interaction.

Removing one copy of CtBP (*CtBP<sup>+/-</sup>*; *Gal4-109-68>ham*), inactivating the CtBP-binding site of Ham (*Gal4-109-68>ham $\Delta$ CtBP*) or a combination of both (*CtBP<sup>+/-</sup>*; *Gal4-109-68>ham $\Delta$ CtBP*) led to reduced socket-to-hair transformations (Fig. 5c and Supplementary Fig. 5b). These data suggest that Ham-mediated modification of Notch activity may occur through the formation a Ham–CtBP transcriptional co-repressor complex.

### Ham controls Notch target activation

To determine whether Ham alters the transcriptional responses of Notch targets, we used two S2 cell variants: S2N cells<sup>24,25</sup> and S2NHam cells. The former express Notch and the latter express both Ham and

**Figure 5** Modification of Notch activity by a Ham–CtBP complex.

(a) Ectopic *ham* expression suppresses Notch signaling in the cell-fate decision between notal-microchaete hair and socket cells. Black arrows indicate normal hair or socket cells. Ectopic expression of *ham* caused either a partial fate conversion (recognized by an ectopic hair-like protrusions on the socket, gray arrow) or a full conversion from socket to hair (white arrows). Scale bar represents 20  $\mu$ m. (b) Bar charts quantifying the fraction of each phenotype on the notum (mean  $\pm$  s.e.m.). The conversion of socket to hair phenotype caused by ectopic Ham was enhanced by removing one copy of *Notch* (*N<sup>55e11</sup>*) (wild type,  $n = 10$  nota, 500 microchaete sensory organs; *N<sup>+/-</sup>*,  $n = 10$  nota, 500 microchaete sensory organs; *109-68>ham*,  $n = 8$  nota, 248 microchaete sensory organs; *N<sup>+/-</sup>*; *109-68>ham*,  $n = 7$  nota, 69 microchaete sensory organs). (c) Fate conversions caused by ectopic Ham were suppressed by removing the Ham CtBP-binding site (*ham $\Delta$ CtBP*) and/or by reducing CtBP levels (*CtBP<sup>87De-10</sup>*) (*CtBP<sup>+/-</sup>*,  $n = 10$  nota, 500 microchaete sensory organs; *109-68>ham*,  $n = 13$  nota, 444 microchaete sensory organs; *CtBP<sup>+/-</sup>*; *109-68>ham*,  $n = 13$  nota, 900 microchaete sensory organs; *109-68>ham $\Delta$ CtBP*,  $n = 10$  nota, 1,134 microchaete sensory organs; *CtBP<sup>+/-</sup>*; *109-68>ham $\Delta$ CtBP*,  $n = 8$ , 1,411 microchaete sensory organs). (d) The domain structure of Ham, mammalian homologs Evi1, Prdm16 and *C. elegans* homolog Egl43. PR, PRD1-BF1 and RIZ homology. (e) A CtBP GST pulldown revealed an interaction between Ham and CtBP. (f) Mutation of the PLDLS sequence to a nonfunctional PLASS sequence led to the loss of this interaction. Lower panels show input controls probed with antibody to V5 (10%) or stained with Coomassie Brilliant Blue (CBB). Full-length blots and gels are presented in Supplementary Figure 6.

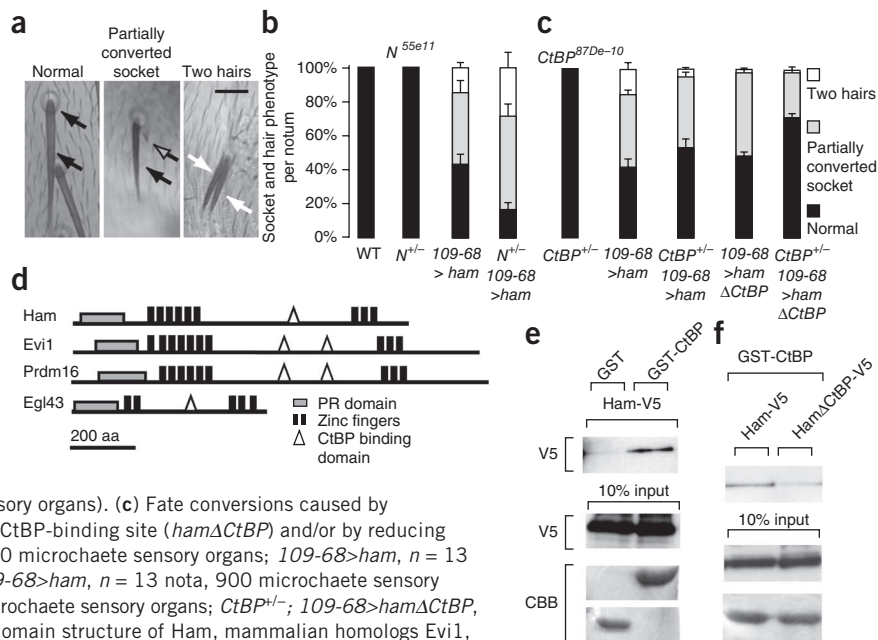
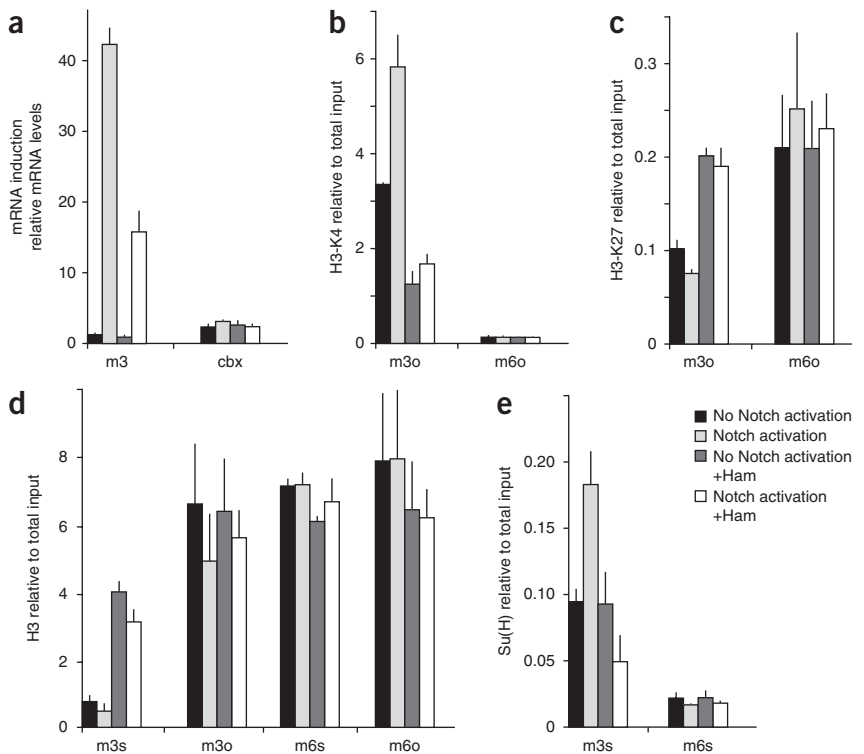


**Figure 6** Ham drives chromatin modification at Notch-target loci. **(a)** mRNA levels for *E(spl)m3* and a control gene (*cbx*). Ham blocked induction of the *E(spl)m3* locus by Notch signaling. A two-way ANOVA analysis highlighted an interaction between Notch signaling state and Ham induction state ( $P = 0.00012$ ). The significance of the effect of Ham induction on the Notch activated state was  $P = 0.00023$ , as determined by a *post-hoc* Tukey test. Data are presented as mean  $\pm$  s.e.m. of target gene expression and chromatin modifications in the absence and presence of Ham (without Notch activation or 30 min after Notch activation). **(b,c)** Trimethylation of H3-K4 **(b)** and H3-K27 **(c)** at *E(spl)m3* and *E(spl)m6* loci measured by ChIP. Independent of Notch, Ham activity suppressed H3-K4 trimethylation ( $P = 0.0015$ , Tukey test) and increased H3-K27 trimethylation at the *E(spl)m3* locus ( $P = 0.00023$ , Tukey test). Data are presented as in **a**. **(d)** Occupancy of histone H3 at the *E(spl)m3* and *E(spl)m6* enhancers (m3s and m6s) or ORFs (m3o and m6o) measured by ChIP. Ham specifically increased H3 occupancy at the *E(spl)m3* enhancer independently of Notch ( $P = 0.00022$ , Tukey test). The levels in the ORF remain unchanged. Data are presented as in **a**. **(e)** Occupancy of Su(H) at the *E(spl)m3* and *E(spl)m6* promoters as measured by ChIP. At the *E(spl)m3* promoter, Ham prevented the increase in Su(H) occupancy that usually occurs after Notch signaling activation. A two-way ANOVA analysis highlighted an interaction between Notch signaling state and Ham induction state ( $P = 0.011$ ). The effect of Ham on the Notch activated state was  $P = 0.0018$  (Tukey test). Data are presented as in **a**.



Notch (Online Methods). In both cells, Notch signaling can be activated by EDTA treatment<sup>24,25</sup> (**Supplementary Fig. 7a**).

In S2N cells, *E(spl)m3* (*enhancer of split m3*) is the primary locus poised for induction by Notch<sup>25</sup>. We examined mRNA expression of *E(spl)m3* and additional control genes that are not Notch targets (*crossbronx* (*cbx*) and *vein*, data not shown)<sup>25</sup> (**Fig. 6a**). Without activation of Notch signaling, no difference was detected in the levels of *E(spl)m3* or control genes either in the presence or absence of Ham. *E(spl)m3* expression was increased 29-fold in S2N cells 30 min after activation of Notch signaling, whereas there was no alteration in the expression of the control genes. On the contrary, Notch-mediated induction of *E(spl)m3* was strongly suppressed in S2NHam cells to 22% of the level in S2N cells; no change was observed in the control genes (**Fig. 6a**).

As we detected locus-specific activity of Ham, we assayed whether there was corresponding selective locus-specific binding. We found selective Ham binding at the Su(H)-binding enhancer of the *E(spl)m3* locus in S2NHam cells regardless of Notch activation state (**Supplementary Fig. 7b**).

Does Ham mediate repression at this promoter level? To test this, we transfected the *E(spl)m3* promoter fused to a luciferase reporter (*E(spl)m3-luc*)<sup>26</sup> into S2 cells. Luciferase expression was increased 11-fold by co-transfection of the NICD. However, activation of this promoter was strongly suppressed following the additional transfection of Ham to only 27% the level of NICD alone. Furthermore, repression of NICD-mediated *E(spl)m3-luc* activation by a Ham zinc finger domain 2 deletion construct<sup>27</sup> was fully dependent on a functional CtBP-binding site (**Supplementary Fig. 7c**). These data suggest that Ham, with CtBP, mediates Notch target transcription.

### Ham drives Notch target chromatin methylation events

Prdm factors may form protein complexes with histone methylation activity<sup>28</sup>. Furthermore, CtBP can act as a bridge to recruit chromatin modification enzymes<sup>29,30</sup>. Such chromatin modifications mediate the ability of genes to respond to inductive signals<sup>31</sup>. We therefore investigated the possibility that Ham could modify Notch signaling via directing chromatin modifications.

The repressive activity of Ham was not altered by treatment with the histone deacetylase inhibitor trichostatin A (data not shown). We asked whether Ham directs histone methylation. Genetic loci that are poised for activation can be discriminated by high levels of trimethylated histone H3-K4 (lysine 4), and loci refractory to induction by high levels of trimethylated H3-K27 (refs. 25,31–33). We examined histone methylation at the *E(spl)m3* open reading frame (ORF) via chromatin immunoprecipitation (ChIP) with chromatin from S2N and S2NHam cells<sup>25</sup> (Online Methods). Ham activity was independent of Notch. Following Ham expression, trimethylation of H3-K4 was suppressed in advance of Notch signaling activation, and the increase in H3-K4 trimethylation that usually occurred following Notch signaling activation was blocked (**Fig. 6b**). In contrast, levels of trimethylated H3-K27 were increased in the presence of Ham regardless of Notch signaling activation (**Fig. 6c**). Finally, transfection of Ham mutant constructs into S2 cells revealed that CtBP-binding site mutations can block this Ham-mediated effect on H3-K27 trimethylation (**Supplementary Fig. 7d**).

### Ham remodels Notch target chromatin

Local histone methylation events are associated with chromatin structural alterations that control accessibility for the transcriptional machinery. In S2N cells, the robust response of *E(spl)m3* to

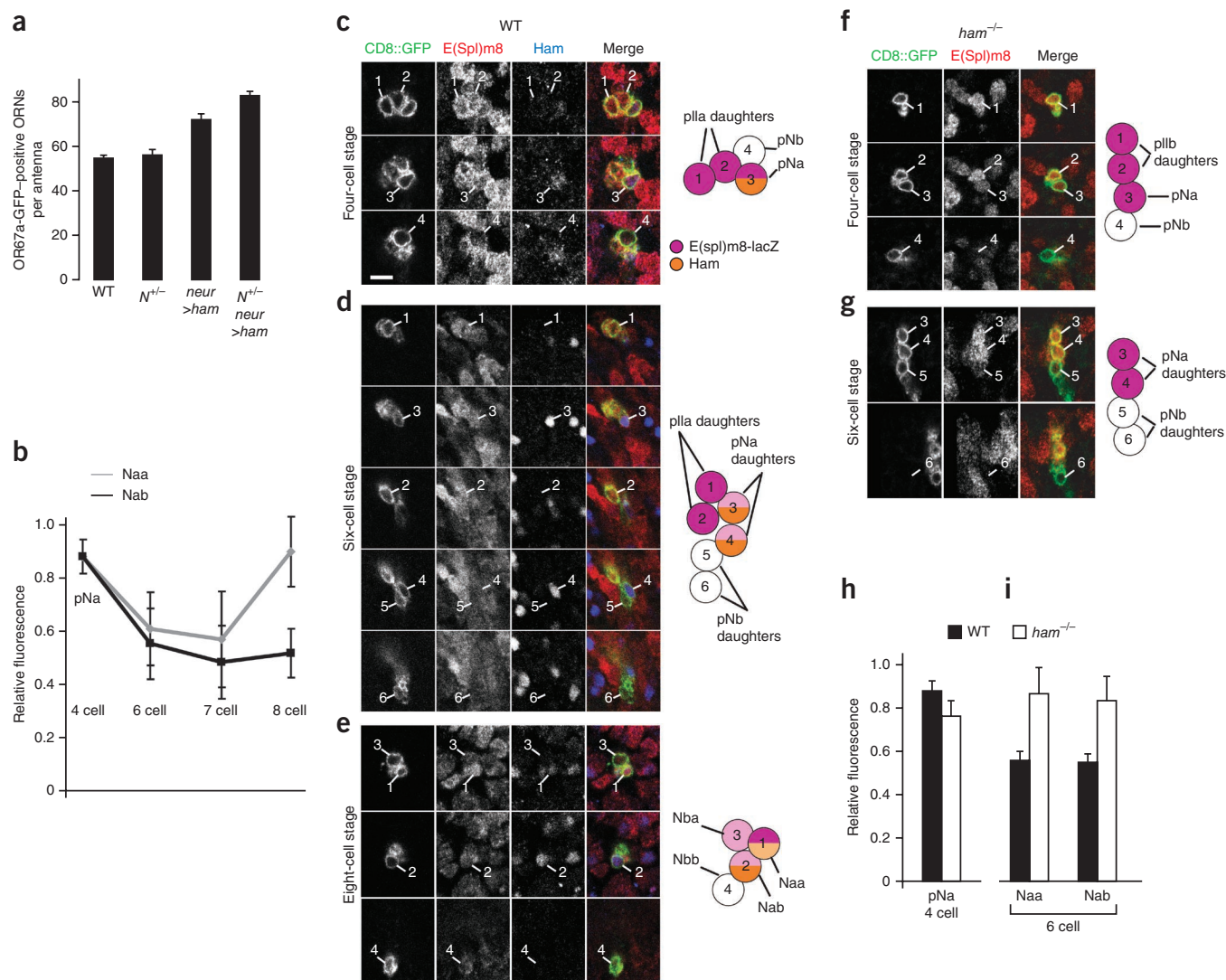


**Figure 7** Ham controls ORN lineage Notch target dynamics. (a) Notch mediates the outcome of ectopic Ham expression on ORN identity (mean  $\pm$  s.e.m.). A two-way ANOVA analysis highlighted an interaction between Notch genotype and ectopic Ham expression state ( $P = 0.036$ ). The Notch genotype altered ORN identity in a Ham overexpression ( $P = 0.00055$ , Tukey test), but not a wild-type ( $P = 0.70$ , Tukey test), background (wild type,  $n = 6$ ;  $N^{+/-}$ ,  $n = 7$ ;  $neur > ham$ ,  $n = 11$ ;  $N^{+/-}; neur > ham$ ,  $n = 9$ ). (b) Quantification of wild-type *E(spl)m8-lacZ* expression in Naa (gray) and Nab (black) clones ( $n = 4, 6, 5$  and  $5$ , for the four-, six-, seven- and eight-cell stages, respectively; mean  $\pm$  s.e.m.). (c–g) Wild-type (c–e) and *ham* (f,g) clones immunostained for  $\beta$ -galactosidase (*E(spl)m8-lacZ*, red), GFP (green) and Ham (blue). In e and g, four and two p11a progeny are out of the focal planes, respectively. Scale bar represents 5  $\mu$ m. (h,i) Quantification of *E(spl)m8-lacZ* expression in wild-type (black) and *ham* (white) clones (mean  $\pm$  s.e.m.). At the four-cell stage, *E(spl)m8-lacZ* levels were the same between wild-type ( $n = 4$ ) and *ham* mutants ( $n = 7$ ;  $P = 0.43$ , unpaired two-tailed Student's *t* test; h). In the wild type at the six-cell stage, *E(spl)m8-lacZ* levels dropped in both Naa and Nab (i). In *ham* mutants, *E(spl)m8-lacZ* levels did not drop; they were 56% higher in wild type than in Naa ( $P = 0.016$ , unpaired two-tailed Student's *t* test; wild type,  $n = 8$  wild type; *ham*,  $n = 7$ ) and 52% higher in Nab ( $P = 0.032$ , unpaired two-tailed Student's *t* test; wild type,  $n = 8$ ; *ham*,  $n = 7$ ).

Notch signaling is a result of low histone density at its Su(H)-binding enhancer<sup>25</sup>. Other members of the *E(spl)* complex have high histone density and were refractory to induction by Notch (Fig. 6d)<sup>25</sup>. Using ChIP, we found that histone H3 levels were low at the *E(spl)m3* enhancer in the absence of Ham, but were increased when Ham was expressed, reaching levels similar to those present at other silent *E(spl)* loci (Fig. 6d).

Induction of Notch target genes is correlated with an increase in Su(H) occupancy at the target enhancer<sup>25</sup>, and this could be affected by chromatin structure. We examined the binding of Su(H) at the *E(spl)m3* enhancer 30 min after Notch signaling activation. Notch signaling activation in the absence of Ham led to a robust increase in

Su(H) occupancy at this enhancer. Induction of Ham in the absence of Notch signaling had no effect on Su(H) occupancy. Notch signaling activation in the presence of Ham, however, revealed that Ham activity blocked the increase in Su(H) occupancy at the enhancer (Fig. 6e). Taken together, these data suggest that Ham regulates transcriptional responses of Notch targets by modifying chromatin accessibility to Su(H).

#### Ham alters Notch target dynamics in the ORN lineage

Does Ham function to mediate Notch signaling *in vivo* during ORN lineage development? Removing one copy of Notch ( $N^{+/-}; neur > ham$ , *tub-Gal80<sup>ts</sup>*) enhanced Ham-mediated promotion of OR67a-positive

identity, suggesting that Ham controls ORN fate *in vivo* by suppressing Notch signaling (Fig. 7a). This Ham function is not a result of control over the asymmetric division machinery, as asymmetric Pon segregation was not affected by *ham* mutation (100%,  $n = 10$ ; Supplementary Fig. 8). This is consistent with our finding that Ham regulates the transcriptional response of Notch targets.

Next, we analyzed whether transcriptional regulation of Notch targets by Ham occurs *in vivo* during ORN lineage development. As no Notch targets have been described in the ORN lineage, we examined the expression of the *E(spl)* genes in the developing antenna using seven available transgenic reporters<sup>10,11</sup>. Only *E(spl)m8* showed an expression pattern that might reflect the differential activation of Notch signaling (Supplementary Table 1).

We analyzed *E(spl)m8-lacZ* and Ham expression in wild-type MARCM clones at sequential stages of ORN lineage elaboration by immunostaining for Ham and  $\beta$ -galactosidase (Fig. 7b–e). *E(spl)m8-lacZ* expression was not observed in the newly born daughters of the pIIb cell (pNa and pNb). At the four-cell stage, it became detectable in pNa along with Ham; neither was expressed in pNb (Fig. 7c). At the six-cell stage, Ham was robustly expressed in both of the pNa daughters (Naa and Nab). In comparison, *E(spl)m8-lacZ* was downregulated in both cells (Fig. 7b,d). At the eight-cell stage, Ham levels were reduced in both cells (Supplementary Fig. 2), whereas *E(spl)m8-lacZ* was upregulated only in Naa (Fig. 7b,e).

To determine whether Ham is involved in the regulation of *E(spl)m8*, we analyzed *E(spl)m8-lacZ* expression in *ham*<sup>-/-</sup> MARCM clones (Fig. 7f,g). At the four-cell stage, both wild-type and *ham*<sup>-/-</sup> clones showed equal levels of *E(spl)m8-lacZ* expression in pNa (Fig. 7h). In addition, at the eight-cell stage, in both *ham*<sup>-/-</sup> and wild-type clones, asymmetric reactivation of *E(spl)m8-lacZ* occurred. We confirmed this in *ham*<sup>-/-</sup> lineages by measuring *E(spl)m8-lacZ* expression; consistently, one pNa daughter showed 84% higher *E(spl)m8-lacZ* expression than the other ( $\pm 29\%$ , s.e.m.,  $n = 7$ ). However, *E(spl)m8-lacZ* expression dynamics were strongly altered in *ham*<sup>-/-</sup> clones in the period between pNa division and *E(spl)m8-lacZ* asymmetric reactivation. At the six-cell stage in wild-type clones, Ham expression was high and *E(spl)m8-lacZ* expression was downregulated in both Naa and Nab. On the other hand, in *ham*<sup>-/-</sup> clones, *E(spl)m8-lacZ* levels did not undergo downregulation and remained more than 50% higher than in wild-type clones in both Naa and Nab (Fig. 7g–i). These data indicate that, in the developing ORN lineage, Ham controls the dynamics of Notch target expression.

## DISCUSSION

Throughout the animal kingdom, a huge number of neuron classes<sup>1</sup> are generated using only a handful of signaling systems<sup>7</sup>. We examined Ham function in the ORN lineage and discovered a mechanism that enables iterative uses of a single intracellular signal to elicit different outcomes. Epigenetic silencing of locus-specific enhancers alters the context of subsequent signaling events.

In mammals, each ORN expresses only one odorant receptor. In *Drosophila*, each ORN usually expresses one odorant receptor, and occasionally expresses two or three<sup>2–5</sup>. Thus, accurately sensing and responding to the odor environment requires an enormous range of ORN classes<sup>5,34,35</sup>. In *Drosophila*, we analyzed the ORN lineage history that gives rise to three primary ORN identities (Naa, Nab and Nba). These three identities arise in a sensillum via iterated rounds of Notch-mediated binary cell-fate decisions. Together with previous findings, our results suggest that diversification of *Drosophila* ORN classes is the result of the combined output of two predominantly hardwired mechanisms; spatially localized factors determine

at least 21 types of sensilla<sup>36–41</sup>, and Notch and Ham then act in each sensillum to maximize ORN class variety.

Biochemical and molecular analyses of Ham function indicate that it can repress Notch target enhancers. In the ORN lineage, Notch signaling is used in consecutive cell fate decisions, and we found that Ham acts to turn off Notch targets before a subsequent round of selective reactivation. We found that Ham was expressed specifically in pNa, the neuronal-intermediate precursor with high Notch activity, and inherited by both of the pNa daughter cells. In addition to our findings, studies in other contexts have observed that some Notch targets require a Notch signal for their transcriptional induction, but not for maintaining their expression<sup>42</sup>. These Notch targets could aberrantly persist in both pNa progeny without the intervention of a mechanism to erase the effects of the preceding Notch signal.

*ham* mutants showed an unusual ORN fate switch. They not only transformed ORN fate with respect to Notch state, but also altered sublineage-specific identity (low-Notch Nab to high-Notch Nba identity). This phenotype suggests that, in addition to suppressing the previous round of Notch activation, Ham may delineate the selection of the next round of targets. As Ham activity resulted in altered chromatin modifications at Notch targets, this suggests that Ham could set an epigenetic context in which the terminal round of Notch signaling occurs.

Although we demonstrated this with respect to Ham, we suggest that this approach to modifying the transcriptional outputs of a signaling pathway may have widespread importance in other lineages that utilize iterative signals. Notch signaling iteration is a widespread phenomenon. One important example is in the maintenance of neural and other stem cells<sup>43</sup>, and it is now known that some chromatin-modifying factors promote stem cell self-renewal<sup>44</sup>. Notably, several Prdm factors have regionalized expression in neural precursor domains of the embryonic mouse spinal cord and could modify and diversify stem cell identity during mammalian CNS development<sup>13</sup>.

In *Drosophila*, Notch signaling and Ham expression are transient in nascent ORNs. Thus, Notch- and Ham-mediated fate choices must be perpetuated during the later selection of alternative axon guidance factors and odorant receptors. It is possible that chromatin methylation not only sets the context of immediate Notch signaling outcomes, but also maintains initial fate choice by priming or silencing promoters for readout during differentiation. The existence of such mechanisms in neural development is now beginning to emerge. It was recently shown that, in mouse cortical precursor cells, the trithorax factor Mixed-lineage leukemia1 (Mll1) prevents epigenetic silencing of the neural differentiation gene *Distal-less homeobox 2* (*Dlx2*), enabling it to be properly upregulated during differentiation stages<sup>45</sup>. In contrast, in the mammalian olfactory system, epigenetic repression is used during the transition from multipotent precursor to immature ORN to silence all ~2,800 odorant receptor genes before subsequent de-repression of a single odorant receptor per neuron<sup>46</sup>.

To determine how chromatin modifications create a context-dependent outcome from signaling and how resultant cell-fate choices are perpetuated during *Drosophila* ORN differentiation, it will be necessary to elucidate the components and action of the chromatin-modification complex targeted by Ham. Furthermore, genome-wide identification of the promoters targeted by Su(H) and Ham will reveal the genes regulated by these factors to confer specific ORN fates.

## METHODS

Methods and any associated references are available in the online version of the paper at <http://www.nature.com/natureneuroscience/>.

Note: Supplementary information is available on the Nature Neuroscience website.

#### ACKNOWLEDGMENTS

We thank L. Luo, T. Hummel, Y. Hiromi, Y.N. Jan, F. Matsuzaki, S. Parkhurst, the Bloomington *Drosophila* Stock Center, Bloomington *Drosophila* Genomics Resource Center, the Iowa Developmental Studies Hybridoma Bank and Flybase for *Drosophila* stocks, DNA clones, antibodies and indispensable database information, and C. Yokoyama and members of the Moore laboratory for advice on the manuscript. Funding was provided by Japan Society for the Promotion of Science Grants-in-Aid Young Scientists (B) to H.T. and Scientific Research (C) to K.E., a RIKEN-Deutscher Akademischer Austauschdienst Research Internship Scholarship to M.S., a Medical Research Council program grant to S.J.B., and a RIKEN Brain Science Institute core award to A.W.M.

#### AUTHOR CONTRIBUTIONS

K.E., M.R.K., E.K., M.S., S.J.B. and A.W.M. carried out genetic analyses. H.T., A.K., E.K. and M.S. carried out molecular biology. K.E., K.I., S.J.B. and A.W.M. wrote the paper. A.W.M. conceived and coordinated the study.

#### COMPETING FINANCIAL INTERESTS

The authors declare no competing financial interests.

Published online at <http://www.nature.com/natureneuroscience/>.

Reprints and permissions information is available online at <http://www.nature.com/reprints/index.html>.

- Stevens, C.F. Neuronal diversity: too many cell types for comfort? *Curr. Biol.* **8**, R708–R710 (1998).
- Vosshall, L.B., Amrein, H., Morozov, P.S., Rzhetsky, A. & Axel, R. A spatial map of olfactory receptor expression in the *Drosophila* antenna. *Cell* **96**, 725–736 (1999).
- Couto, A., Alenius, M. & Dickson, B.J. Molecular, anatomical, and functional organization of the *Drosophila* olfactory system. *Curr. Biol.* **15**, 1535–1547 (2005).
- Fishilevich, E. & Vosshall, L.B. Genetic and functional subdivision of the *Drosophila* antennal lobe. *Curr. Biol.* **15**, 1548–1553 (2005).
- Mori, K. & Sakano, H. How is the olfactory map formed and interpreted in the mammalian brain? *Annu. Rev. Neurosci.* **34**, 467–499 (2011).
- Louvi, A. & Artavanis-Tsakonas, S. Notch signaling in vertebrate neural development. *Nat. Rev. Neurosci.* **7**, 93–102 (2006).
- Pires-daSilva, A. & Sommer, R.J. The evolution of signaling pathways in animal development. *Nat. Rev. Genet.* **4**, 39–49 (2003).
- Endo, K., Aoki, T., Yoda, Y., Kimura, K. & Hama, C. Notch signal organizes the *Drosophila* olfactory circuitry by diversifying the sensory neuronal lineages. *Nat. Neurosci.* **10**, 153–160 (2007).
- Bray, S. & Bernard, F. Notch targets and their regulation. *Curr. Top. Dev. Biol.* **92**, 253–275 (2010).
- Cooper, M.T. *et al.* Spatially restricted factors cooperate with Notch in the regulation of Enhancer of split genes. *Dev. Biol.* **221**, 390–403 (2000).
- Kramatschek, B. & Campos-Ortega, J.A. Neuroectodermal transcription of the *Drosophila* neurogenic genes *E(spl)* and *HLH-m5* is regulated by proneural genes. *Development* **120**, 815–826 (1994).
- Swanson, C.I., Evans, N.C. & Barolo, S. Structural rules and complex regulatory circuitry constrain expression of a Notch- and EGFR-regulated eye enhancer. *Dev. Cell* **18**, 359–370 (2010).
- Kinameri, E. *et al.* Prdm proto-oncogene transcription factor family expression and interaction with the Notch-Hes pathway in mouse neurogenesis. *PLoS ONE* **3**, e3859 (2008).
- Moore, A.W., Jan, L.Y. & Jan, Y.N. *hamlet*, a binary genetic switch between single- and multiple- dendrite neuron morphology. *Science* **297**, 1355–1358 (2002).
- Moore, A.W., Roegiers, F., Jan, L.Y. & Jan, Y.N. Conversion of neurons and glia to external cell fates in the external sensory organs of *Drosophila hamlet* mutants by a cousin-cousin cell-type respecification. *Genes Dev.* **18**, 623–628 (2004).
- Lu, B., Rothenberg, M., Jan, L.Y. & Jan, Y.N. Partner of Numb colocalizes with Numb during mitosis and directs Numb asymmetric localization in *Drosophila* neural and muscle progenitors. *Cell* **95**, 225–235 (1998).
- Hayashi, S. *et al.* GETDB, a database compiling expression patterns and molecular locations of a collection of Gal4 enhancer traps. *Genesis* **34**, 58–61 (2002).
- Andrews, H.K., Giagtzoglou, N., Yamamoto, S., Schulze, K.L. & Bellen, H.J. Sequoia regulates cell fate decisions in the external sensory organs of adult *Drosophila*. *EMBO Rep.* **10**, 636–641 (2009).
- Wang, S., Younger-Shepherd, S., Jan, L.Y. & Jan, Y.N. Only a subset of the binary cell fate decisions mediated by Numb/Notch signaling in *Drosophila* sensory organ lineage requires Suppressor of Hairless. *Development* **124**, 4435–4446 (1997).
- Abdelilah-Seyfried, S. *et al.* A gain-of-function screen for genes that affect the development of the *Drosophila* adult external sensory organ. *Genetics* **155**, 733–752 (2000).
- Kajimura, S. *et al.* Regulation of the brown and white fat gene programs through a PRDM16/CtBP transcriptional complex. *Genes Dev.* **22**, 1397–1409 (2008).
- Izutsu, K. *et al.* The corepressor CtBP interacts with Evi-1 to repress transforming growth factor beta signaling. *Blood* **97**, 2815–2822 (2001).
- Palmer, S. *et al.* Evi-1 transforming and repressor activities are mediated by CtBP co-repressor proteins. *J. Biol. Chem.* **276**, 25834–25840 (2001).
- Rand, M.D. *et al.* Calcium depletion dissociates and activates heterodimeric Notch receptors. *Mol. Cell Biol.* **20**, 1825–1835 (2000).
- Krejci, A. & Bray, S. Notch activation stimulates transient and selective binding of Su(H)/CSL to target enhancers. *Genes Dev.* **21**, 1322–1327 (2007).
- Mukherjee, A. *et al.* Regulation of Notch signaling by non-visual beta-arrestin. *Nat. Cell Biol.* **7**, 1191–1201 (2005).
- Seale, P. *et al.* Transcriptional control of brown fat determination by PRDM16. *Cell Metab.* **6**, 38–54 (2007).
- Völkel, P. & Angrand, P.O. The control of histone lysine methylation in epigenetic regulation. *Biochimie* **89**, 1–20 (2007).
- Shi, Y. *et al.* Coordinated histone modifications mediated by a CtBP co-repressor complex. *Nature* **422**, 735–738 (2003).
- Chinnadurai, G. Transcriptional regulation by C-terminal binding proteins. *Int. J. Biochem. Cell Biol.* **39**, 1593–1607 (2007).
- Mikkelsen, T.S. *et al.* Genome-wide maps of chromatin state in pluripotent and lineage-committed cells. *Nature* **448**, 553–560 (2007).
- Bernstein, B.E. *et al.* Methylation of histone H3 Lys 4 in coding regions of active genes. *Proc. Natl. Acad. Sci. USA* **99**, 8695–8700 (2002).
- Schneider, R. *et al.* Histone H3 lysine 4 methylation patterns in higher eukaryotic genes. *Nat. Cell Biol.* **6**, 73–77 (2004).
- Suh, G.S. *et al.* A single population of olfactory sensory neurons mediates an innate avoidance behavior in *Drosophila*. *Nature* **431**, 854–859 (2004).
- Kurtovic, A., Widmer, A. & Dickson, B.J. A single class of olfactory neurons mediates behavioral responses to a *Drosophila* sex pheromone. *Nature* **446**, 542–546 (2007).
- Ray, A., van Naters, W.G., Shiraiwa, T. & Carlson, J.R. Mechanisms of odor receptor gene choice in *Drosophila*. *Neuron* **53**, 353–369 (2007).
- Bai, L., Goldman, A.L. & Carlson, J.R. Positive and negative regulation of odor receptor gene choice in *Drosophila* by Acj6. *J. Neurosci.* **29**, 12940–12947 (2009).
- Tichy, A.L., Ray, A. & Carlson, J.R. A new *Drosophila* POU gene, *pdm3*, acts in odor receptor expression and axon targeting of olfactory neurons. *J. Neurosci.* **28**, 7121–7129 (2008).
- Komiyama, T., Carlson, J.R. & Luo, L. Olfactory receptor neuron axon targeting: intrinsic transcriptional control and hierarchical interactions. *Nat. Neurosci.* **7**, 819–825 (2004).
- Chou, Y.H., Zheng, X., Beachy, P.A. & Luo, L. Patterning axon targeting of olfactory receptor neurons by coupled hedgehog signaling at two distinct steps. *Cell* **142**, 954–966 (2010).
- Gupta, B.P. & Rodrigues, V. *atonal* is a proneural gene for a subset of olfactory sense organs in *Drosophila*. *Genes Cells* **2**, 225–233 (1997).
- Bray, S. & Furiols, M. Notch pathway: making sense of suppressor of hairless. *Curr. Biol.* **11**, R217–R221 (2001).
- Pierfelice, T.J., Schreck, K.C., Eberhart, C.G. & Gaiano, N. Notch, neural stem cells, and brain tumors. *Cold Spring Harb. Symp. Quant. Biol.* **73**, 367–375 (2008).
- He, S., Nakada, D. & Morrison, S.J. Mechanisms of stem cell self-renewal. *Annu. Rev. Cell Dev. Biol.* **25**, 377–406 (2009).
- Lim, D.A. *et al.* Chromatin remodeling factor *Mll1* is essential for neurogenesis from postnatal neural stem cells. *Nature* **458**, 529–533 (2009).
- Magklara, A. *et al.* An epigenetic signature for monoallelic olfactory receptor expression. *Cell* **145**, 555–570 (2011).

## ONLINE METHODS

**Genetic analyses.** All of the wild-type and mutant clones were generated using the MARCM technique as described previously<sup>8</sup>. To analyze cell fate-specific gene expression or *E(spl)*-*lacZ* expression in the ORN lineage, we induced clones using *hs-flp* with a 37 °C heat shock given at 48–33 h before puparium formation for 30 min, and we dissected the developing antennae at 21–23 h after puparium formation (APF). The genotypes of the animals were *w Gal4-C155 hs-flp/w* or *Y; FRT<sup>G13</sup>UAS-mCD8::GFP/FRT<sup>G13</sup>tubP-Gal80* (wild type), *w Gal4-C155 UAS-mCD8::GFP/w* or *Y; m8-lacZ/UAS-mCD8::GFP; tubP-Gal80 FRT2A/FRT2A* or *w Gal4-C155 UAS-mCD8::GFP/w* or *Y; m8-lacZ FRT40A/tubP-Gal80 FRT40A; UAS-mCD8::GFP* (*m8-lacZ* expression in wild type), and *w Gal4-C155 UAS-mCD8::GFP/w* or *Y; ham<sup>1</sup> m8-lacZ FRT40A/tubP-Gal80 FRT40A; UAS-mCD8::GFP* (*m8-lacZ* expressions in *ham<sup>1</sup>*).

To label daughters of either pNa or pNb, clones were induced using *hs-flp* with a 37 °C heat shock given for 15 min at 12–15 h APF, and the adult brains were dissected from the 3–5-d-old flies. The genotype of the flies was *w Gal4-C155 hs-flp/w* or *Y; FRT<sup>G13</sup>UAS-mCD8::GFP/FRT<sup>G13</sup>tubP-Gal80*.

To analyze the axonal projections of ORNs labeled by *Gal4-NP0724*, we induced clones using *ey-flp* and dissected pupal brains at 45–96 h APF. The genotypes of the flies were *y w ey-flp/w* or *Y; FRT<sup>G13</sup> UAS-mCD8::GFP/FRT<sup>G13</sup> tubP-Gal80; Gal4-NP0724/UAS-mCD8::GFP*.

To analyze the axonal projection of ORNs homozygous for *ham<sup>1</sup>*, we induced clones using *hs-flp* with a 37 °C heat shock given for 30 min at 48–0 h before puparium formation, and dissected the adult brains from 3–5-d-old flies. The genotype of flies were *w Gal4-C155 hs-flp UAS-mCD8::GFP/w* or *Y; ham<sup>1</sup> FRT40A/tubP-Gal80 FRT40A; UAS-mCD8::GFP* or *y w hs-flp/w* or *Y; Gal4-AM29 ham<sup>1</sup> FRT40A/tubP-Gal80 FRT40A; UAS-mCD8::GFP/+*. To examine Svp expression in the *GAL4-NP0724*-positive cells, we dissected antennae from flies carrying *GAL4-NP0724* and *UAS-mCD8::GFP* during the pupal stage (21 h APF).

To analyze odorant receptor expression in *ham* mutant antenna, we crossed *ham<sup>1</sup> FRT40A/CyO, Dfd-GMR-YFP; Or67a-mCD8::GFP* (or other relevant odorant receptor promoter-*mCD8::GFP* fusion lines<sup>3</sup>)/*TM6B, Tb* to *Df(2)ED1195/CyO, Dfd-GMR-YFP*. For overexpression, *UAS-ham neur-Gal4, tubP-Gal80<sup>ts</sup>/TM6B, Tb* was crossed to *Or67a-mCD8::GFP* or other relevant odorant receptor promoter-*mCD8::GFP* fusion lines<sup>3</sup>. We examined the interaction of Notch in a *N<sup>55e11</sup>/+* background. To ectopically express Ham, we used a temperature shift from 18 °C to 29 °C at 19 APF (at 18 °C) and maintained the flies at 29 °C for 4 h before returning them to 18 °C for the rest of pupation.

To examine the genetic interaction of ectopic *ham* expression with other genes in the bristle lineage, we crossed *Gal4-109-68; UAS-ham/TM6B, Tb tubP-Gal80* to *N<sup>55e11</sup>* or *N<sup>1</sup>* or *N<sup>264-40</sup>/FM7, B*; *CtBP<sup>87De-10</sup>* or *CtBP<sup>03436</sup>/TM6B, Tb*; *Su(H)<sup>SF8</sup>* or *Su(H)<sup>AR9</sup>/CyO*, *GMR-Dfd-YFP* or *yw* and Oregon-R controls. To make *hamΔCtBP*, we mutated the nucleic acid sequence encoding the CtBP-binding site from CCGTTGGACCTT TCC (PLDLS) to CCGTTGGCCTCTTCC (an inactive PLASS<sup>22,23</sup>) by site-directed mutagenesis. *hamΔZF2* was made by truncating immediately before the second domain of Zinc fingers (amino acid 935), and *hamΔCtBPAZF2* is a combination of the two. To ensure our experimental conclusions were not biased by insertion effects, we generated and tested many independent transgenic lines for each construct<sup>12</sup>. Flies were raised at 18 °C until white pupae and then switched to 29 °C for the rest of development. Notae were dissected, mounted in Hoyer's reagent, and the socket and hair phenotypes were quantified under bright-field illumination at 40× (Nikon E80i).

**Immunohistochemistry.** Brains and antennae were fixed with 4% paraformaldehyde (wt/vol) in phosphate-buffered saline for 70 min and 40 min, respectively, and immunostained with a standard method. For primary antibodies, we used rabbit antibody to GFP (1:500, Molecular Probes), rat antibody to GFP (1:1,000, Nacalai Tesque), mouse antibody to GFP (1:100, Roche), rabbit antibody to β-galactosidase (1:3,000, Cappel), mAb nc82 (1:50)<sup>47</sup>, rat antibody to Elav (1:250, 7E8A10, Developmental Studies Hybridoma Bank (DSHB)), mouse antibody

to Elav (1:100, 9F8A9, DSHB), antibody to Pon (1:500)<sup>16</sup>, antibody to Ham (1:100)<sup>14</sup>, antibody to Svp (1:5)<sup>48</sup>, rat antibody to Pros (1:50)<sup>49</sup>, antibody to Cut (1:50, 2B10, DSHB). Optical sections of a specimen were collected using a Zeiss LSM510 or a Leica SP2 confocal microscope.

The *m8-lacZ* expression in the ORN lineage was quantified by measuring mean optical density in the largest area of each cell belonging to a SOP clone through optical sections using ImageJ (US National Institutes of Health). All the measurements were normalized by measurement of pNb (four-cell stage) or averaged value of measurements of pNb daughters (other stages) for each clone.

**Cell culture and molecular biology.** Full-length *ham* cDNA<sup>14</sup> was cloned into pMT/V5-HisA (Invitrogen) and stably introduced into S2N cells<sup>25</sup> by standard methods to make S2NHam cells. In S2N cells, EDTA treatment forces the cleavage of the Notch extracellular domain as a result of a conformational change caused by deprivation of extracellular calcium ions. This leads to a consequent rapid nuclear accumulation of the NICD<sup>24,25</sup>. Induction of *Notch* and *ham* gene expression by CuSO<sub>4</sub>, EDTA-mediated Notch signaling activation, measurements of the target gene mRNA level and ChIP analyses were all carried out using previously described methods, primer sets and antibodies: histone H3 (Abcam), trimethyl K4 (Abcam), trimethyl K27 (Upstate), Su(H) (Santa Cruz)<sup>25</sup>. All of the experiments were carried out in triplicate for each treatment. Ham ChIP was carried out of S2NHam cells using an antibody to V5 via standard protocols and using previously described primer sets<sup>25</sup>. For analysis of Ham deletion constructs, the relevant plasmids were transfected into S2 cells.

Co-immunoprecipitation was carried out using standard procedures with hemagglutinin-tagged full-length *CtBP* cDNA (DGRC) cloned into pRMHA5 and co-transfected into S2 cells with pMT-*ham*-V5. GST pulldown was performed using standard methods. Ham-V5 or HamΔCtBP-V5 proteins were incubated with GST-CtBP. Bound complexes were separated by SDS-PAGE, transferred onto PVDF and detected using antibody to V5. For liquid chromatography-mass spectrometry analysis, nuclear extracts from Ham-V5-overexpressing S2 cells were incubated with antibody to V5 overnight at 4 °C. Protein G beads were incubated with the nuclear extracts for 3 h at 4 °C. After the beads were washed four times with a buffer containing 150 mM KCl, a standard trypsin digestion method was applied. The proteins recovered from the digestion were analyzed by mass spectrometry (Linear Ion trap Mass Spectrometer, LTQ, Thermo Fisher Scientific) and subsequent data via Mascot (Matrix Science); the alpha level was set at 0.05.

For examination of *E(spl)m3* promoter activity via a luciferase reporter (*E(spl)m3-luc<sup>26</sup>*), S2 cells were plated at an initial density of 5 × 10<sup>4</sup> cells per well and transfected 24 h later with the relevant combination of NICD and Ham constructs. Culture medium was changed with 1 mM CuSO<sub>4</sub> containing medium 4 h after transfection, and luciferase activity was measured 24 h later using the Promega luciferase assay system as per manufacturer's instructions.

**Statistical analysis.** Statistical analysis of immunohistological analysis was by unpaired, two-tailed Student's *t* test (Fig. 4), or two-way ANOVA with *post hoc* Tukey tests (Fig. 7). Statistical analysis of immunoprecipitation data was carried out by two-way ANOVA with *post hoc* Tukey tests (Fig. 6). For all tests, the alpha level was set at 0.05.

47. Wagh, D.A. *et al.* Bruchpilot, a protein with homology to ELKS/CAST, is required for structural integrity and function of synaptic active zones in *Drosophila*. *Neuron* **49**, 833–844 (2006).

48. Kanai, M.I., Okabe, M. & Hiromi, Y. *seven-up* controls switching of transcription factors that specify temporal identities of *Drosophila* neuroblasts. *Dev. Cell* **8**, 203–213 (2005).

49. Matsuzaki, F., Koizumi, K., Hama, C., Yoshioka, T. & Nabeshima, Y. Cloning of the *Drosophila prospero* gene and its expression in ganglion mother cells. *Biochem. Biophys. Res. Commun.* **182**, 1326–1332 (1992).